CATEGORY: Real-World Applications

EVALUATION OF GENETIC PROGRAMMING AND NEURAL NETWORKS TECHNIQUES FOR NUCLEAR MATERIAL IDENTIFICATION

Sara Pozzi
Department of Nuclear Engineering
Polytechnic of Milan
Milan, Italy
Tel. +39 02 2399 6340
e-mail: pozzi@ipmce7.cesnef.polimi.it

Javier Segovia✉
Facultad de Informática
Universided Politecnica de Madrid
Madrid, Spain
Tel. +34 91 3367451
e-mail: fsegovia@fi.upm.es

✉ **Contact Person**

Abstract

Nuclear materials safeguard efforts necessitate the use of non-destructive methods to determine the attributes of fissile samples enclosed in special, non-accessible containers. To this end, a large variety of methods has been developed. Usually, a given set of statistics of the stochastic neutron-photon coupled field, such as source-detector, detector-detector cross correlation functions, and multiplicities are measured over a range of known samples to develop calibration algorithms. In this manner, the attributes of unknown samples can be inferred by the use of the calibration results.

The sample identification problem, in its most general setting, is then to determine the relationship between the observed features of the measurement and the sample attributes and to combine them for the construction of an optimal identification algorithm. The goal of this paper is to compare a combination of genetic algorithms and neural networks (NN) with genetic programming (GP) for this purpose. To this end, the time-dependent MCNP-DSP Monte Carlo code has been used to simulate the neutron-photon interrogation of sets of uranium metal samples by a 252Cf-source. The resulting sets of source-detector correlation functions, R12(•) as a function of the time delay, • , served as a data-base for the training and testing of the algorithms.

1 INTRODUCTION

Nuclear materials safeguard necessitates the use of non-destructive methods to determine the attributes of fissile samples enclosed in special, non-accessible containers. To this end, a large variety of methods has been developed at the Oak Ridge National Laboratory (ORNL) and elsewhere (Mihalczo et al., 1997) (Krick et al., 1992). Active non-destructive assay evolved based on the use of an interrogation source emitting neutrons and gamma rays, whose scope is that of inducing fission in the fissile material within the sample. Neutrons and gamma rays from the source as well as those eventually emitted by the fissile system are then measured with appropriate detectors.

In particular, the 252Cf noise analysis method, currently adapted at the Instrumentation and Controls Division of the Oak Ridge National Laboratory, evolved as a combination of randomly pulsed neutron measurements and Rossi-α measurements. The method consists in collecting the times of each spontaneous fission event from the source as well as the detection times, thus allowing the computation of time-dependent signatures. Previous measurements and Monte Carlo simulations have shown the sensitivity of these signatures (for instance source-detector and detector-detector time-dependent cross-correlation functions, as well as multiplicity measurements) to fissile mass.

The analysis is performed by means of a set of measurements of the time-dependent signatures in a range of known samples. The attributes of unknown samples can then be inferred by resorting to these calibration results. The sample identification problem, in its most general setting, is to determine the relationship between the observed features of the measurement and the sample attributes and to combine them for the construction of an effective identification algorithm.

The goal of this paper is to develop an artificial intelligence approach to this problem whereby Neural Networks and Genetic Programming algorithms are used for sample identification purposes. To this end, a number of Monte Carlo simulations (Valentine, 1997) were performed to obtain source-detector cross-correlation functions for a set of uranium metal samples of different shapes, masses, and enrichments.

The results found serve as a proof of principle for the application of combined stochastic and artificial intelligence methods to safeguards procedures.

The organization of the paper is as follows: Section 2 is a description of the Monte Carlo simulations performed with cylindrical and spherical uranium metal samples. Section 3 identifies a number of features extracted from the time-dependent cross-correlation functions. Sections 4 and 5 describe the use of the two approaches. In the first, a neural network is combined with a genetic algorithm to optimize the network's values of learning rate and momentum. In the second approach genetic programming is used. In both cases explicit expressions linking the features to the quantities of interest (sample mass and enrichment) are found. Section 6 compares the obtained results, and in section 7 the conclusions are shown

The results obtained show that both the neural network and the genetic programming algorithms are robust in predicting the mass and enrichment of uranium metal samples. These values were estimated with very good approximation in both the set used for training and in that used for testing (mean error of about .03 kg in the mass prediction, and 1% in the enrichment prediction).

2 ^{252}CF-SOURCE-DRIVEN SIMULATIONS

In the ^{252}Cf-source-driven measurement the source undergoes spontaneous fission emitting neutrons and gamma rays. The timing of each spontaneous fission event is recorded in appropriate time bins. If fissile material is present inside the sample to be analyzed, the neutrons emitted by the source will initiate fission chains. Neutrons and gamma rays from the source as well as those eventually emitted by the fissile system are measured with two detectors. The detection times are also recorded, in time bins of 1 ns. The uranium sample to be analyzed is placed between the source and two fast plastic scintillation detectors. The source was located at 25.4 cm from the center of the uranium metal sample at a height of 10 cm. The detectors, 10.16 cm width and height and 5.08 cm thick, are placed one on top of the other at a distance of 25.4 cm from the center of the sample.

Simulations were performed with cylindrical and spherical samples of seven different masses (8 kg, 10 kg, 12 kg, 14 kg, 16 kg, 18 kg, and 20 kg). The different masses were obtained by increasing the sample radius, both in the case of the cylinders (in which case the height was kept constant at 20 cm) and in that of the spheres. For each mass, four different enrichments were tested ranging from depleted to highly enriched (0.2 wt% ^{235}U, 36.0 wt% ^{235}U, 50.0 wt% ^{235}U, and 93.15 wt% ^{235}U). Two additional simulations were run for both cylinders and spheres giving a total of 30 simulations for the cylindrical samples and 30 for the spherical ones. An additional simulation run with no sample between source and detectors will be referred to as the void simulation.

The source-detectors cross-correlation functions [$R_{12}(\tau)$] were generated by correlation of the source signal with the combined signal from the two detectors, and normalizing to the source count rate to remove the dependence on the source.

3 SELECTION OF FEATURES FOR THE SAMPLE IDENTIFICATION ALGORITHM

The selection of features for the sample identification algorithm (SIA) was performed on the basis of their relationship to sample attributes and of their ability to discriminate between close numerical values within each attribute group. The first feature (F_1) chosen is the integral of the cross-correlation function at time lags from 0 to 8 ns, normalized to the same integral of the void calculation. It essentially corresponds to the normalized area of the first peak of the cross-correlation function and depends only on the sample mass (see figure 1).

The second feature chosen (F2) is the integral of the cross-correlation function at time lags from 0 to 100 ns, normalized to the same integral of the void simulation. F_2 is sensitive to both the sample's total mass and enrichment (figure 2). The average delay time was selected as the third feature (F3). This feature is

essentially constant for the depleted samples, increases with sample enrichment and for high enrichments is very sensitive to sample mass (figure 3). Because the asymmetry of the second peak of the cross-correlation function is generated by the neutron induced fission in the sample, the skewness of the cross correlation function was selected as feature (F4) (figure 4).

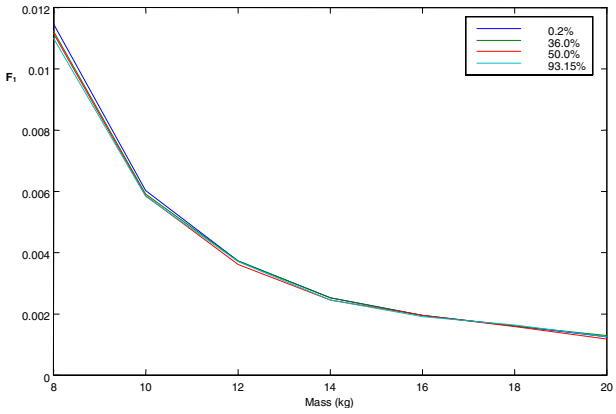

Fig. 1. Cylindrical samples: F_1 as a function of sample mass (kg) for the four different enrichments.

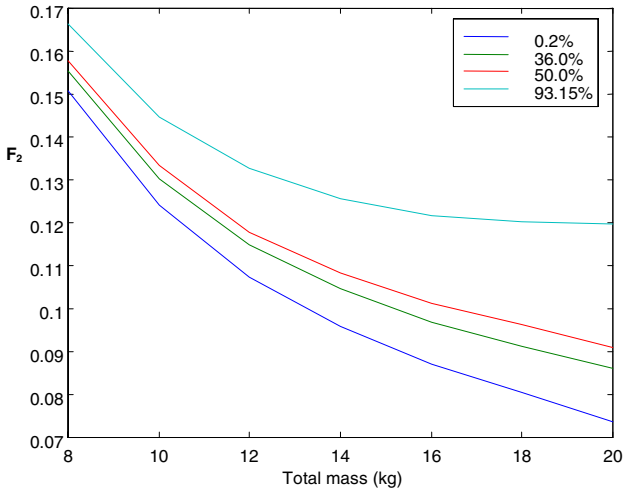

Fig. 2 Cylindrical samples: F_2 as a function of sample mass (kg) for the four different enrichments.

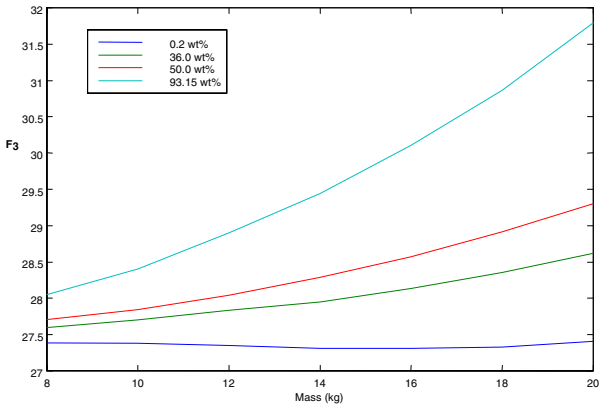

Fig. 3. Cylindrical samples: F_3 as a function of sample mass (kg) for the four different enrichments

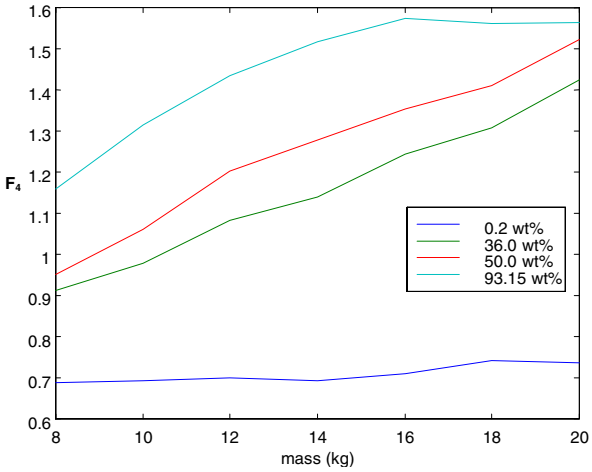

Fig. 4. Cylindrical samples: F_4 as a function of sample mass (kg) for the four different enrichments

4 NN APPLIED TO THE PREDICTION OF THE SAMPLE TOTAL MASS AND ^{235}U ENRICHMENT

Two three-layered artificial neural networks (Marseguerra et al. 1992) (Urig, 1991) were trained to generate a mapping from input (F_1, F_2, F_3, and F_4) to output. One network mapped sample's mass and and the other the enrichment. The well known error back-propagation algorithm was used for the network's training. The activation functions were chosen to be sigmoidal from the input to the hidden layer and linear from the hidden layer to the output. The number of hidden nodes was set to two.

For each NN, the values of learning rate and momentum for the training were optimized by a genetic algorithm (GA) (Chambers, 1995) as shown in Figure 5. In the GA an initial population of 50 chromosomes, each made up of two genes coding the quantities of interest, is allowed to evolve according to the rules of mating, cross-over, and mutation, similarly to what occurs in biological systems. The objective is to maximize the fitness function, defined as the inverse of the network's training error. After a predetermined number of generations (100 in our case), the fittest chromosome is selected.

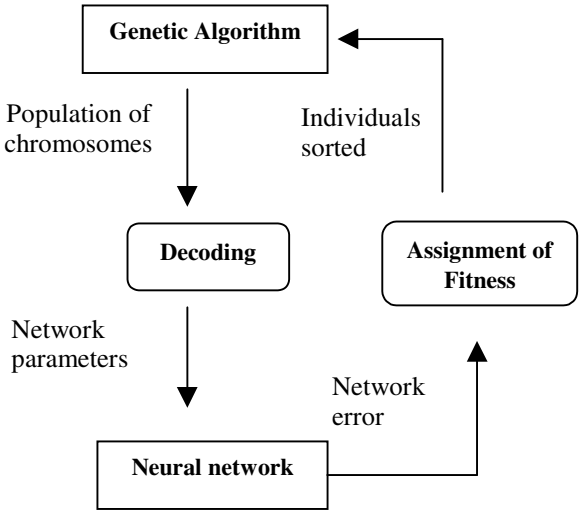

Figure 5: GA-NN combinated operation

The values of learning rate and momentum selected as described above were then used in training the neural networks for the prediction of the total mass and enrichment of the samples on the basis of the four features F_1-F_4.

4.1 RESULTS

Having chosen a linear transfer function in the output nodes of the NN allows us to express the network mapping structure in terms of the simple analytical formula below:

$$Output = \frac{a_1}{1 + e^{-\sum_{i=1..4} b_i F_i + b_5}} + \frac{a_2}{1 + e^{-\sum_{i=1..4} c_i F_i + c_5}} + a_3$$

where a_i, (i=1,2,3), b_j, c_j, (j=1,…5) are coefficients which depend on the network's weights, and the output is the sample mass or enrichment.

19 simulations, about two thirds of the data available, were selected for the NN training. The NN were tested with the remaining 11 cases. The results are shown in Figures 6 and 7. Inspection of these results shows that the present type of neural network can predict enrichment and mass values for uranium metallic samples to a very good approximation both in the case of the training patterns and in the test cases.

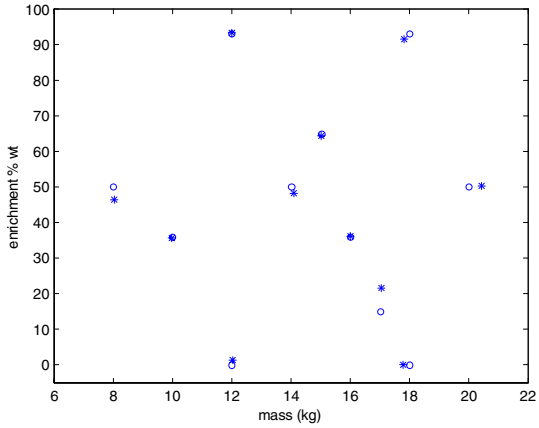

Fig. 6. Neural network prediction of mass and enrichment on the basis of features F_1, F_2, F_3, and F_4: test set of 11 cases relative to cylinder simulations. The true values are shown with the circles and the values predicted by the network with stars.

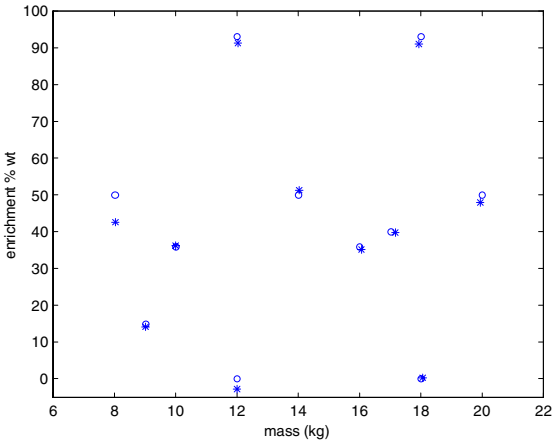

Fig. 7. Neural network prediction of mass and enrichment on the basis of the features F_1, F_2, F_3, and F_4: test set of 11 cases relative to sphere simulations. The true values are shown with the circles and the values predicted by the network with stars.

5 GP APPLIED TO THE PREDICTION OF THE SAMPLE TOTAL MASS AND ^{235}U ENRICHMENT

A Steady State GP algorithm (Banzhaf et al. 1998) was applied to generate a mapping of the features, F_1, F_2, F_3, and F_4, to the sample mass and enrichment. The parameters of the algorithm were as follows:

a) Terminal set: F_1, F_2, F_3, and F_4, normalized in [-1, +1], and random constants in (-01., +0.1). A normalization of the output was also done. It is important to note that the normalization was not necessary for the cylinder's data, but on the contrary it was almost mandatory for the sphere's in order to get good results. Random constants were selected with a probability of 28%, while each F_i with 9%.

b) Function set: operators +,-,*,/ (protected), selected with equal probabilities of 9%. The accumulative probability of selection between terminals and functions in a genetic operation is 100%.

c) Population size: 10,000.

d) Maximum initial size for trees (step 1 of the algorithm): 4 nodes.

e) Maximum size for trees after any genetic operator: 50 nodes.

f) Termination criterion: -0.001 error or 100,000 iterations. It is important to note that the criterion based on the number of iterations, which is the criterion that says that the population of trees cannot be improved in its present configuration and a restart should be done, it is unlikely reached in these experiments.

g) Tournament size: 7. The replacement of bad elements is done within the entire population.

h) Probabilities for selecting genetic operators: reproduction 7%, mutation 20%, crossover 73%.

Training and test sets were similar to those used in section 4.

5.1 RESULTS

The following equations show one example of results obtained for each sample (note that the features and desired outputs were normalized). We got many of them with an acceptable error and this selection was not made under any objective criteria.

Cylinder:

```
Mass = (((((F1 - -0,514) * ((F1 - ((((F1 * F1) - F1) + -0,876) / (-0,502 + -0,584))) * -0,58)) * -0,582) * -0,574) - (((-0,876 - F1) + ((F1 * ((((F1 * F1) - F1) + -0,882) / (-0,49 + -0,544))) * (F1 * F1))) / (-0,498 + -0,59)))

Enrichment = (((F4 - (-0,014 * (F4 - (-0,014 / F4)))) - (((F2 * 0,748) * ((F3 * 0,366) + (F4 - (-0,014 / ((F1 + ((F4 - (-0,014 / (F2 - (F4 * F3)))) - (-0,014 * F4))) - (F4 * (F3 / 0,748)))))))) * F3)) + F2)
```

Sphere:

```
Mass = ((-0,204 * ((F2 * (((-0,49 * ((F4 - -0,722) - (F2 * ((-0,49 / -0,88) + F2)))) * (-0,45 / ((((F3 * F2) * ((F2 * F2) - F2)) * ((F3 * -0,722) - F2)) - F2))) - F2)) - F3)) - F2)

Enrichment = ((((-0,5 + (F4 + (F2 * (F4 - F3)))) * F2) * (F4 * -0,742)) - ((F4 * -0,49) + ((((F4 + F2) - (-0,496 + ((F4 - ((((F4 - F3) - -0,81) * ((F4 - F3) * (F4 + F2))) * F4)) * -0,49))) + F2) * -0,54)))
```

Figures 8 and 9 show their application to the test set. After inspection of the above equations, it can be found that:

a) Mass for the cylinder is calculated using just F1. This simplification can be found in most of the solutions. The explanation of this result is that the cylinder intercepts most of the source photons, thus, the area under the photo peak, normalized to the same area for the void run, is a measure of the photon attenuation that depends on the sample mass. Because for cylinders, the F_1 feature depends so strongly on the mass of the sample (see section 3), the GP program selected just F_1 among the four inputted features.

b) Mass for the sphere is calculated using just F_2 and F_3. We have found this kind of simple dependence in many other solutions. The spherical sample intercepts less photons than in the case of the cylindrical sample, thus, F_1 does not contain too much sample mass information. The F_2 feature, on the contrary, contains the mass information from the photo peak (F_1), plus the sensitivity to sample mass imprinted in the left side of the second peak. The third feature, F_3, is also selected by the program for its high sensitivity to sample mass at high sample enrichments.

For both spherical and cylindrical samples, the equations constructed by the GP algorithm to determine the sample enrichment depend only on the F_2, F_3, and F_4 features because of the F_1 feature exclusive dependence on sample mass.

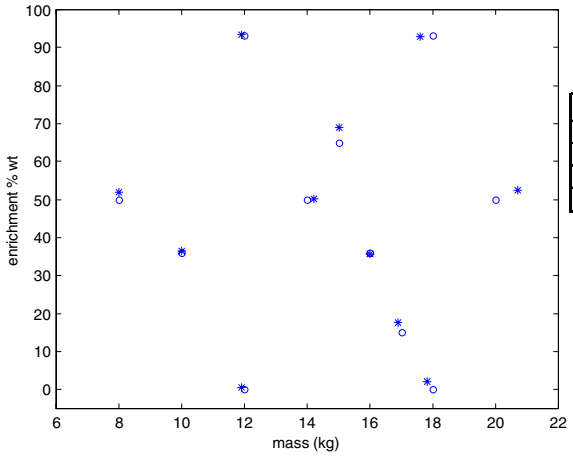

Fig. 8. Genetic Programming: prediction of mass and enrichment on the basis of features F_1, F_2, F_3 and F_4: set of 11 cases used for testing relative to Cylinder simulations. The true values are shown with the circles and the values predicted by the algorithm with stars.

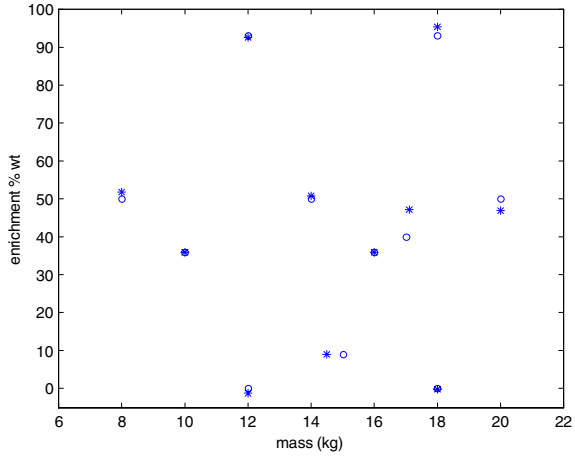

Fig.9. Genetic Programming: prediction of mass and enrichment on the basis of features F_1, F_2, F_3 and F_4: set of 11 cases used for testing relative to Sphere simulations. The true values are shown with the circles and the values predicted by the network with stars.

6 COMPARISON OF RESULTS

In order to make a more meaningful comparison of the results we applied a Standard Regression to predict the mass and enrichment of the cylindrical and spherical samples. Tables 1 and 2 summarize the error for the three techniques for both training and test cases. The error measure used was:

$$Error = \frac{\sum_i \left| real_i - predicted_i \right|}{\sum_i real_i}$$

Cylinder	PREDICTED BY GP		PREDICTED BY NN		PREDICTED BY Regression	
	MASS	ENRICH	MASS	ENRICH	MASS	ENRICH
Training	0.71%	1.67%	0.22%	2.07%	3.05%	14.81%
Test	1.34%	2.16%	0.81%	2.14%	2.69%	12.68%
Extra	0.45%	8.18%	0.13%	9.05%	1.87%	10.52%

Table 1: Error results for the cylindrical samples.

Sphere	PREDICTED BY GP		PREDICTED BY NN		PREDICTED BY Regression	
	MASS	ENRICH	MASS	ENRICH	MASS	ENRICH
Training	0.17%	2.95%	0.27%	2.20%	1.95%	21.37%
Test	0.15%	2.38%	0.27%	4.59%	2.18%	14.71%
Extra	0.38%	14.00%	0.72%	13.33%	1.08%	43.40%

Table 2: Error results for the spherical samples.

The tables show that GA-NN and GP are comparable and more effective than a regression in solving the prediction problem. GA-NN and GP are capable of dealing with non-linear problems and this is demonstrated in the case of the enrichment for both configurations, cylinder and sphere, in which the linear solution, the regression, performs very poorly, indicating that the problem is strongly non-linear.

We have found non remarkable differences in the performance between GA-NN and GP techniques. Two cases (rows labeled as 'Extra' samples in the tables 1 and 2) of the test sets had enrichment values selected outside of the training set range, that can be used to test the overfitting of the models. The error in predicting these enrichment values range from 8% to 14%, far larger than the error produced with the other values, indicating that some overfit has taken place. This can be explained by considering that there were only four values of enrichment in the training set, covering a wide range of enrichment: from depleted to highly enriched uranium. Better results can be obtained by adding more cases to the training set.

7 CONCLUSIONS

Monte Carlo simulations of the source-detector cross correlation function for various sample shapes, mass, and enrichment values have been performed to serve as a training set for two artificial intelligence algorithms (AI): neural networks (NN) and genetic programming (GP). The input presented to the AI algorithm has been in the

form of features extracted from the physical properties of the cross-correlation functions related to mass (beam attenuation) and to enrichment (fission induced pulse broadening). Both the NN and GP algorithms have shown good capabilities and robustness for mass and enrichment predictions of uranium metal samples.

These results serve as a proof of principle for the application of combined stochastic and AI methods to safeguards procedures.

Acknowledgments

We would like to thank R. B. Perez, T. E. Valentine, J. T. Mihalczo, and J. K. Mattingly for their suggesting the topic and for providing help for the use of the MCNP-DSP Monte Carlo Code. Many thanks go to Matteo Cantoni for his help in the implementation of the neural network-genetic algorithm approach and to Professor Marzio Marseguerra for his valuable intellectual contribution and experienced guidance. Both these individuals are from the Politecnico, Milano, Italy. One of us, Sara Pozzi, would like to express her gratitude towards the staff of the Instrumentation and Controls Division for their help and kindness during her stay at the Oak Ridge National Laboratory. Part of this work was supported by the Comision Interministerial de Ciencia y Tecnología of Spain with the grant TIC97-2016-CE.

References

J. T. Mihalczo, T. E. Valentine, J. A. Mullens, and J. K. Mattingly, Report Number Y/LB-15,946 R3, September 26, 1997.

M. S. Krick, D. G. Langner, et. al., *Nuclear Material Management* (Proc. Issue) XXI, 779 (1992).

T. E. Valentine, "MCNP-DSP Users Manual", ORNL/TM-13334, Oak Ridge Nat. Lab, January 1997.

M. Marseguerra, S. Minoggio, A. Rossi, and E. Zio, "Artificial Neural Networks Applied to Multiple Signals in Nuclear Technology," *Progress in Nuclear Energy*, Vol. 27, 4 (1992).

R. E. Urig, "Potential Application of Neural Networks to the Operation of Nuclear Power Plants," *Nuclear Safety*, Vol. 32, 1 (1991).

L. Chambers, *Practical Handbook of Genetic Algorithms – Applications,* CRC Press (1995).

W. Banzhaf, P. Nordin, R. E. Keller, and F. D. Francone, *Genetic Programming: An Introduction* (1998).